

# The NEAR X-Ray/Gamma-Ray Spectrometer

*John O. Goldsten*

**T**he X-Ray/Gamma-Ray Spectrometer on the Near Earth Asteroid Rendezvous (NEAR) spacecraft will remotely sense X-ray and gamma-ray emissions from the surface of near-Earth asteroid 433 Eros and look for characteristic "signatures" in those emissions to determine its elemental composition. During the planned 10 months of orbits about Eros beginning in early 1999, data returned from the instrument will be used to develop global maps of the asteroid, including the content and variations of its surface composition, thereby providing important clues about its nature and origin. (Keywords: Gamma-ray, NEAR, Spectrometer, X-ray.)

## INTRODUCTION

The Near Earth Asteroid Rendezvous (NEAR) mission was launched on 17 February 1996. NEAR is the first spacecraft under NASA's Discovery Program, an initiative for small, low-cost planetary missions. As the first to orbit an asteroid, NEAR promises to answer fundamental questions about the nature and origin of near-Earth objects.

Launched from a Delta II rocket, the 805-kg NEAR spacecraft will follow a  $\Delta V$  Earth-gravity-assisted trajectory and take approximately 3 years to reach 433 Eros, one of the largest near-Earth asteroids.<sup>1,2</sup> This trajectory also provided a flyby of main-belt asteroid 253 Mathilde in June 1997.

During the planned 10 months at Eros, a suite of remote sensing instruments will make detailed science observations of the gross physical properties, surface composition, and morphology of the asteroid. Four months of the rendezvous are scheduled with orbits as low as 35 km, corresponding to altitudes as low as 15 km above the asteroid surface.

The X-Ray/Gamma-Ray Spectrometer (XGRS), one of five major instruments on the NEAR spacecraft, is the primary experiment for determining the surface and near-surface elemental composition of Eros. Other instruments in the science payload include the Multispectral Imager (MSI), Near-Infrared Spectrometer (NIS), Magnetometer, and NEAR Laser Rangefinder. The MSI will image the surface morphology of Eros with spatial resolutions down to 5 m. The NIS will be the primary instrument for measuring mineral abundances with a spatial resolution on the order of 300 m. The combined observations of the XGRS, MSI, and NIS should provide full coverage of Eros, yielding global maps of its surface composition.

The XGRS is a complex instrument with little design heritage. To meet the strict schedule constraints of the Discovery Program, the successful development of the XGRS required a focused team working closely with other NEAR instrument teams. Formal work on XGRS began in December 1993. The fully tested and

calibrated instrument was delivered to the NEAR spacecraft in August 1995, a development time of less than 22 months.

## X-RAY AND GAMMA-RAY SPECTROSCOPY: THE MEASUREMENT TECHNIQUE

The XGRS is a remote sensing instrument. From orbits of 35 to 100 km, it remotely senses the characteristic X-ray and gamma-ray emissions from the asteroid surface. Remote sensing of this type is only possible for bodies with little or no atmosphere to absorb these emissions. Orbital, rather than flyby, missions are preferred for such measurements because of the typically long observation times required. The XGRS is designed to have sufficient sensitivity to distinguish between major meteorite types and will either identify the type of meteorite to which Eros is linked or confirm the absence of a relationship.<sup>3</sup>

X-ray spectroscopy from an orbiting spacecraft can be used to identify elemental composition at the surface of an airless body in the following manner.<sup>4,5</sup> X-rays from the Sun shining on Eros will produce significant X-ray fluorescence from the elements contained in the very surface of the asteroid (the top 1 mm). When an element fluoresces, it emits X-rays with discrete energies that are unique or characteristic of that element (the strongest being K $\alpha$  X-rays). The asteroid-pointing portion of the X-Ray Spectrometer (XRS) detects these characteristic X-rays in the 1- to 10-keV energy range. From an analysis of the measured energy spectrum, elemental composition can be inferred.

Although the intensity of detected X-rays is a strong function of solar illumination and activity, the expected returns should be sufficiently intense to measure the surface abundances of elements Mg, Al, Si, Ca, and Fe with spatial resolutions down to 2 km. To ensure a proper quantitative analysis, XRS points two additional X-ray detectors sunward to directly measure the incident solar flux. XRS signal strength will, in general, improve as the Sun approaches solar maximum and will be particularly strong during the random solar flares that produce brief periods of high-level, high-energy solar X-rays.

Remote gamma-ray spectrometry provides a complementary measure of near-surface elemental composition.<sup>6-8</sup> The Gamma-Ray Spectrometer (GRS) detects discrete-line gamma-ray emissions in the 0.1- to 10-MeV energy range. In this range, spectroscopy can be used to measure the abundance of O, Si, Fe, and H, which become excited or activated (radioactive) owing to continual bombardment by galactic cosmic rays. In addition, it can detect the presence of the naturally radioactive elements K, Th, and U. Unlike the low-energy X-rays, gamma rays are not as easily absorbed and therefore can escape from regions

beneath the top surface. This allows the GRS to probe deeper than the XRS to a surface depth on the order of 10 cm.<sup>3</sup>

Solar illumination does not significantly affect the gamma-ray coverage of the asteroid, but the generally weak gamma-ray emissions require the GRS to have a wide field of view and to integrate for long periods of time to achieve sufficient sensitivity to determine elemental abundances quantitatively. Therefore, the GRS has very limited spatial resolution, perhaps only 5 to 10 pixels, characterizing the entire asteroid. However, to the extent that X-rays and gamma rays can be compared for the same element, differences in measured concentrations by the X-ray and gamma-ray experiments should reveal the depth and extent of a dust layer (regolith) on the asteroid.<sup>3</sup>

## INSTRUMENT OVERVIEW

The philosophy of NEAR was to conceive a comprehensive science mission that could answer fundamental questions about the nature and origin of near-Earth asteroids while meeting the schedule and cost constraints of the Discovery Initiative. To that end, the spacecraft has the necessary sophistication to achieve the mission goals (e.g., a three-axis-stabilized platform), yet also has the attributes of a simple, robust design with its fixed high-gain antenna and solar panels.

This philosophy translated to the science instruments as well. All instruments are fixed to the spacecraft and rely on a passive thermal design. For the GRS, this setup excluded the use of an elaborate cryogenically cooled detector mounted on a boom in the manner of Mars Observer.<sup>6</sup> For the XRS, high cost and development time excluded the use of detectors made of solid beryllium like those used on Apollo.<sup>9,10</sup> Despite these constraints, the XGRS contains a suitable complement of detectors that possess the reliability to survive a long-duration mission and provide sufficient sensitivity and resolution to measure and map the surface composition of Eros.

The XGRS is partitioned as several assemblies of detectors, electronics, and a cabling harness. These components are distributed over three deck surfaces of the NEAR spacecraft (Fig. 1). The asteroid-pointing X-ray and gamma-ray detector assemblies are mounted next to each other on the aft deck along with the other science instruments. Nearby are detector electronics that contain all of the analog signal processing functions. Behind the detector electronics package is a dedicated data processing unit (DPU), which executes all instrument software, provides the digital interface to the spacecraft, and supplies instrument power and control.

Two additional X-ray detectors sit atop the forward deck so they can monitor the solar X-ray flux. Knowledge of the input flux is required for quantitative

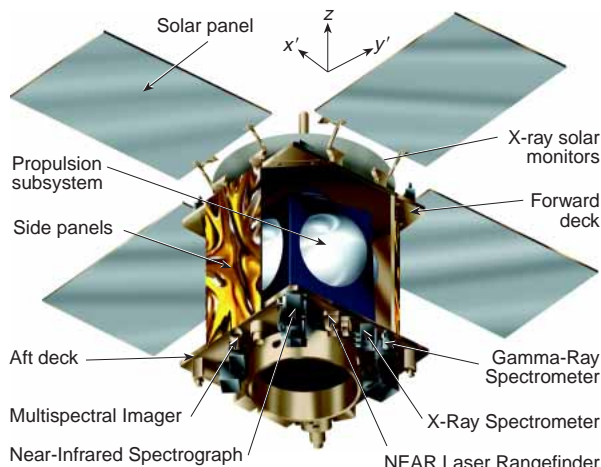


**Figure 1.** View of the NEAR spacecraft. The aft deck contains the instrument palette and is almost completely in shadow. The spacecraft  $z$  axis is directed through the high-gain antenna, which is nominally pointed toward Earth. Instruments are oriented so that their boresights are nearly coaligned with the  $x'$  axis. The two X-ray solar monitors (not visible) reside on the forward deck to always face toward the Sun within  $30^\circ$ .

analysis of the X-ray spectra from the asteroid.<sup>4</sup> The solar monitors' fields of view are normal to the solar panels and are located above one corner of the deck so that they are not obscured by the high-gain antenna. The spacecraft is generally oriented with its high-gain antenna directed toward Earth. With this orientation, the Sun is always within  $30^\circ$  of the central axis of the spacecraft.

For reliability, each of the seven XGRS detectors has its own high-voltage power supply. The supplies are divided into three stacks located on the inside surface of the aft deck. A separate electronics module to control the high-voltage supplies is mounted atop the detector electronics package.

The XGRS instrument (Fig. 2) has a total mass, including the DPU, of 27 kg and dissipates a maximum of 34 W. The power system allows power switching of the high-voltage subsystem, thermoelectric cooler, and operational heaters.

The NEAR spacecraft's solid-state recorders and downlink are limited resources, and their use and

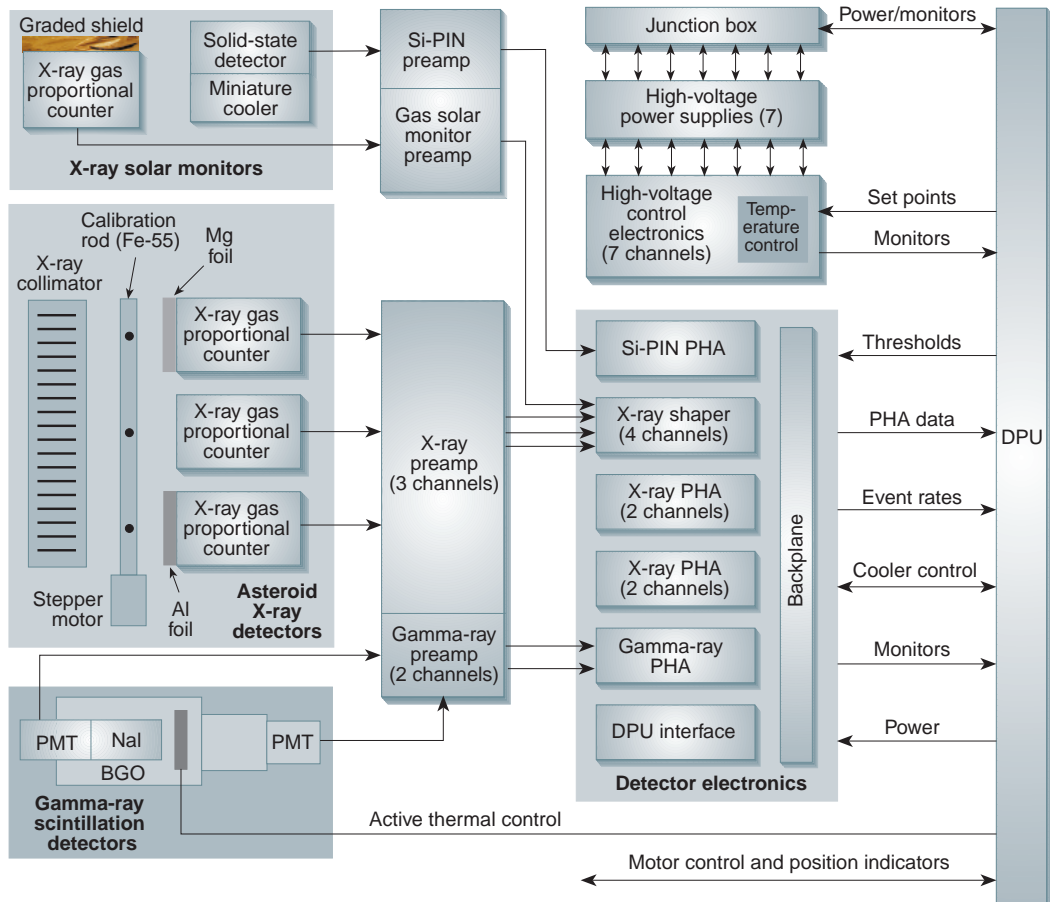


**Figure 2.** Functional block diagram of the XGRS including the asteroid-pointing X-ray gas proportional counters, gamma-ray scintillation detectors (BGO and NaI) with photomultiplier tubes (PMT), shared preamp module, Si-PIN photodiode and gas proportional counter solar monitors with their associated preamps, and the central detector electronics box, which contains the pulse shapers and pulse-height analyzers (PHA). Spectra are formed in the data processing unit (DPU), which also provides the spacecraft interface.

allocation are regularly negotiated throughout the mission. Telemetry data rates for the XRS and GRS are independently adjustable and may be raised or lowered by commanding shorter or longer integration periods from 60 to 60,000 s. In this way, the XGRS can easily respond to changes in telemetry allocation. At Eros, the expected telemetry rates for the GRS and XRS will nominally be 70 and 180 bits/s, respectively. An added summary science mode provides a reduced set of highly compressed spectra from both experiments and combines them into a single data stream with a telemetry rate of only a few bits per second. This mode is particularly useful for checking the health and safety of the instrument and for verifying its operating configuration.

Both spectrometers are energy-dispersive rather than wavelength-dispersive systems. For this type of instrument (Fig. 3), a single incoming photon is absorbed by the detector material (solid or gaseous) and produces an output signal proportional to the energy absorbed. The output signal is generally in the form of a charge pulse, which may last from a few nanoseconds to several hundred nanoseconds. A charge-sensitive preamplifier collects the charge from the detector and produces a voltage step proportional to the total amount of charge. A linear filter network then amplifies and shapes the preamplifier signal to reduce noise and provide a smooth signal more suitable for "pulse-height" analysis, a process in which the peak value of each pulse is measured using an analog-to-digital converter. The DPU collects these measurements and bins

them according to pulse height or energy absorbed. After an appropriate accumulation time, in which many photons are processed, a complete pulse-height distribution or energy spectrum is accumulated and telemetered to Earth. From an analysis of the telemetered spectrum, elemental composition can be inferred.

Timing circuits detect the arrival of photons whenever the energy signals exceed a commandable threshold, which is generally set just above the noise level of the electronics. The timing circuits also detect the near-simultaneous arrival of photons (random, independent events) that generate a condition called pile-up and corrupt the energy measurements. Pile-up rejection logic automatically discards these events to ensure the highest-quality data.

This generalized detection scheme forms the basic approach to the design of the XGRS. Additional techniques are employed to reduce unwanted background signals, enhance sensitivity, and provide long-term stability and in-flight calibration. Table 1 summarizes the important characteristics and specifications of the instrumentation.

## INSTRUMENT DESIGN

### Gamma-Ray Spectrometer

As noted previously, restrictions on mass, cost, and mission duration precluded the use of the type of gamma-ray detector on Mars Observer, which was a cryogenically cooled, high-purity Ge detector mounted on an extended boom to remove it from the local background radiation of the spacecraft. Instead, the NEAR GRS employs an NaI(Tl) (thallium-activated sodium iodide) scintillator mounted within a cup shield made of bismuth germanate (BGO). The dense BGO cup is itself an active scintillator and thus works to reduce the Compton and pair-production contributions to the unwanted background signal. In addition, it provides direct, passive shielding from the local gamma-ray environment. This design eliminates the need for a boom and allows the detector to be body-mounted to the spacecraft.

The gamma-ray detector subassembly (Fig. 4) was designed and built by EMR Photoelectric, a division of Schlumberger. The central detector assembly is based on a ruggedized NaI(Tl) unit used in oil well logging operations. The BGO cup was designed especially for NEAR and is fabricated from a single crystal. The mass of the complete detector assembly is 6 kg.

Scintillation detectors produce a light intensity proportional to the energy absorbed with a wavelength that is characteristic of the detector material. The NaI(Tl) and BGO crystals each optically couple to a photomultiplier tube (PMT) equipped with an optimized photocathode to convert its light output to

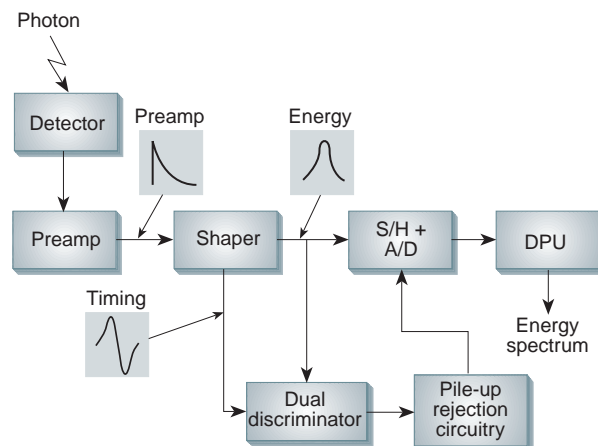


**Figure 3.** Generalized detection scheme for the XGRS. A single photon is absorbed in a detector and produces an electrical signal proportional to the energy. The electrical signal is amplified and shaped into a pseudo-Gaussian pulse. The peak value is captured by a sample and hold (S/H) circuit and measured by an analog-to-digital (A/D) converter. Energy measurements are passed to a data processing unit (DPU) where they are histogrammed to form an energy spectrum. The discriminator is triggered whenever the signal is above the electronics noise level. Pile-up rejection circuitry disallows analysis of photon events spaced too closely in time for an accurate measurement.

Table 1. Instrument characteristics.

Component	Specifications
GRS	
Prime detector	NaI(Tl) scintillator, $2.54 \times 7.62$ cm
Shield detector	BGO <sup>a</sup> scintillator cup, $8.9 \times 14$ cm
Energy range	0.1 to 10 MeV, 1024-channel spectra
NaI(Tl) energy resolution	8.7% fwhm <sup>b</sup> @ 662 keV
BGO <sup>a</sup> energy resolution	14% fwhm @ 662 keV
Field of view	$\approx 50^\circ$ fwhm @ 145 keV
Anticoincidence background rejection	>500:1 above 5 MeV
Counting rate	10 kHz maximum (1 kHz nominal)
Mass	6 kg
XRS	
X-ray detectors (3)	Single-wire gas-filled proportional counters
Window	25- $\mu$ m beryllium with 2-mm grid support
Active aperture area	25 cm <sup>2</sup> per detector
Energy range	0.5 to 10 keV, 256-channel spectra
Energy resolution	850 eV fwhm @ 5.9 keV
Collimator	Small-cell honeycomb, Be-Cu foil
Field of view	$5^\circ$ fwhm @ 5.9 keV
Rise time rejection of background	>50% above 2 keV; >70% @ 6 keV
Counting rate	10 kHz maximum (1 kHz nominal)
In-flight calibration sources	Fe-55; rotated into field of view by command
X-ray solar monitors	
Energy range	1 to 10 keV, 256-channel spectra
Field of view	60°
Counting rate	10 kHz (strong solar flare)
Redundant detectors	
Gas-filled proportional counter	Graded shield design; 1 mm <sup>2</sup> equivalent area
Solid-state detector	Si-PIN photodiode, 1.1 $\times$ 1.1 mm, mounted on miniature thermoelectric cooler
Energy resolution	Gas: 850 eV fwhm @ 5.9 keV PIN: 600 eV fwhm @ 5.9 keV

<sup>a</sup>Bismuth germanate.<sup>b</sup>Full width at half maximum.

electrical signals and provide a signal gain of roughly 100,000. Crystal and PMT combinations were carefully chosen by EMR to achieve the best energy resolution.

The measured energy resolutions for the NaI(Tl) and BGO detectors mounted in the flight configuration are 8.7% and 14% full width at half maximum (fwhm), respectively, at an energy of 662 keV (the standard gamma-ray calibration line of Cs-137). The presence of the small PMT between the NaI crystal and the incident gamma rays introduces a small but

characterizable loss in sensitivity for the NaI detector that is a function of both energy and angle.<sup>3</sup>

The flight spare detector exhibits nearly identical performance and will be used extensively throughout the mission to further characterize detector performance and develop a detector model. Although the energy resolution of a NaI(Tl) scintillator is not nearly as good as that of a cooled Ge detector,<sup>8</sup> the NEAR detector operates at room temperature, is not subject to any serious radiation damage (important for long-duration missions such as NEAR), and, given the

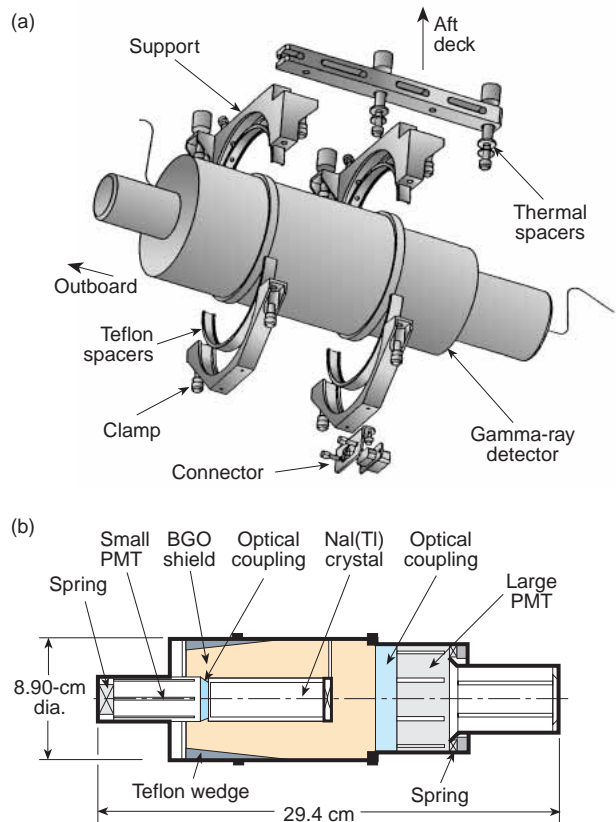


**Figure 4.** NEAR gamma-ray detector: (a) sensor assembly; (b) detector cross section showing central NaI(Tl) detector situated within an active BGO cup shield to reduce unwanted background signals by almost 3 orders of magnitude. The photomultiplier tubes (PMTs) at each end convert the light output of the scintillation detectors into electrical signals.

integration times planned for the mission, meets the measurement requirements for the elements cited previously.

Temperature and voltage stability are extremely important to maintain system performance. The light outputs of the NaI(Tl) and BGO scintillators vary significantly with temperature. Temperature fluctuations during asteroid operations would adversely affect detector calibration, so the detector assembly is thermally isolated and wrapped with operational heaters to stabilize the gamma-ray detector temperature to within  $0.25^{\circ}\text{C}$ . The signal gains of the PMTs are not particularly sensitive to temperature, but are very sensitive to voltage variations. The PMT high-voltage power supplies must be stable to a fraction of a volt over temperature so as not to adversely affect GRS calibration. To meet this requirement, the XGRS uses an external feedback control system to produce ultra-stable high-voltage outputs from ordinary high-voltage power supplies.

The cup shield acts as an active collimator. Particles or gamma rays entering through the shield will produce

output signals in the shield detector that are coincident with signals produced in the central detector. An anticoincidence system detects and rejects these events. The cup design confines the field of view to about  $45^{\circ}$  at lower energies. At higher energies, the field of view is somewhat larger.<sup>3</sup>

With this detector configuration, much of the composition signal is lost at higher energies owing to pair production. One or both of the gamma rays produced by annihilation will probably escape the small central crystal and be absorbed in the shield. This energy loss appears in the raw NaI spectrum as secondary peaks shifted down in energy from the photopeak by either 0.511 or 1.022 MeV, named the first and second escape peaks, respectively. In the anticoincidence spectrum, these escape peaks are suppressed because of event rejection by the anticoincidence system.

For many gamma rays of interest, more events are contained in the first and second escape peaks than in the photopeak itself, and rejection of these events would cause an unacceptable loss in sensitivity. To recover this information, the GRS watches for any coincident events with shield energies falling near 0.511 or 1.022 MeV and produces two additional spectra containing only these types of events. Although these coincidence modes are somewhat vulnerable to false detections arising from galactic cosmic rays and Compton scattering, extensive testing and calibration have demonstrated the overall improvement in performance using this new technique.<sup>3</sup>

Extensive ground calibrations were performed on the GRS using various radioactive sources.<sup>3</sup> For in-flight energy calibration, the GRS relies on prominent spectral lines such as the 511-keV annihilation line and others generated by the activation of the NaI(Tl) and BGO crystals due to galactic cosmic-ray bombardment. Periodic instrument calibrations obtained during the cruise to Eros and in orbit will be validated using ground-based measurements on the flight spare detectors and will be compared with measurements from the other NEAR instruments and Earth-based observations. Figure 5 shows pulse-height spectra obtained in flight from the GRS.

#### X-Ray Spectrometer

The XRS consists of three identical gas-filled proportional counters designed and built by Metorex International Oy of Finland. Gas tubes of this type provide the large active area and therefore the sensitivity required for remote sensing. Similar detectors have been flown on lunar orbital missions and most recently on Apollo missions 15 and 16.<sup>4,10,11</sup> The NEAR XRS uses an updated design and achieves an energy resolution of 850 eV fwhm at 5.9 keV. The energy range of the detectors extends from 0.5 to 10

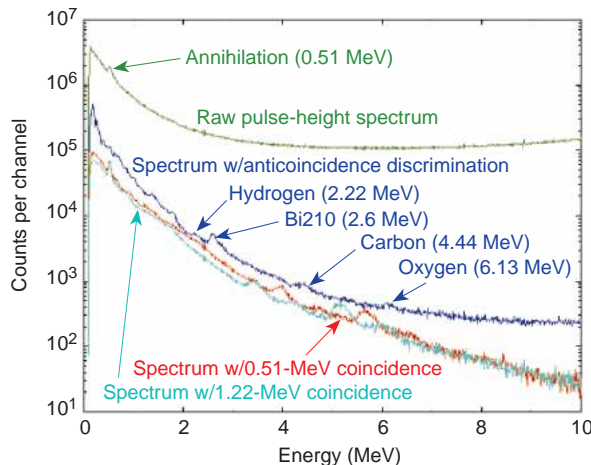


**Figure 5** Background spectra obtained in flight with the NEAR NaI detector. The accumulation time is approximately 38 days. The anticoincidence spectrum reveals structure that cannot be observed in the raw spectrum.

keV. Figure 6 shows an exploded view of the major mechanical assemblies of the X-ray sensor.

The gas proportional counters are similar to the gamma-ray detectors in that they detect individual photons. An incoming X-ray photon penetrates the thin window of a sealed gas-filled chamber and interacts with the gas, producing an energetic photoelectron (the photoelectric effect). The kinetic energy of the electron is then progressively absorbed in the gas, leaving an ionization trail. The free electrons from the ionization are attracted to a thin wire anode at high potential stretched down the center of the chamber. In the region of high electric field strength, very close to the wire, the electrons reach sufficient energy to liberate even more electrons in a stable multiplication effect that provides signal gain. This signal gain helps to overcome the preamplifier noise such that the energy resolution of the gas tubes is primarily limited by the Poisson statistics of the ionization process.

Occasionally, an incoming X-ray photon with sufficient energy will interact with an inner-shell electron of the gas (primarily argon for the XRS). In this case, the resulting photoelectron is less energetic than expected owing to the significant energy required for ionization. Eventually, a nearby free electron will "fall" into the ionized atom, resulting in the emission of an X-ray with an energy characteristic to argon (3 keV). Usually, this argon X-ray is quickly reabsorbed in the gas, and so the total energy measured by the detector remains unchanged. However, if the argon X-ray escapes the gas tube without being absorbed, the measured energy will appear lower by the escaped amount. This overall effect produces "escape" peaks in the spectra that are downshifted in energy by 3 keV from the primary peaks, and with intensities roughly 10%

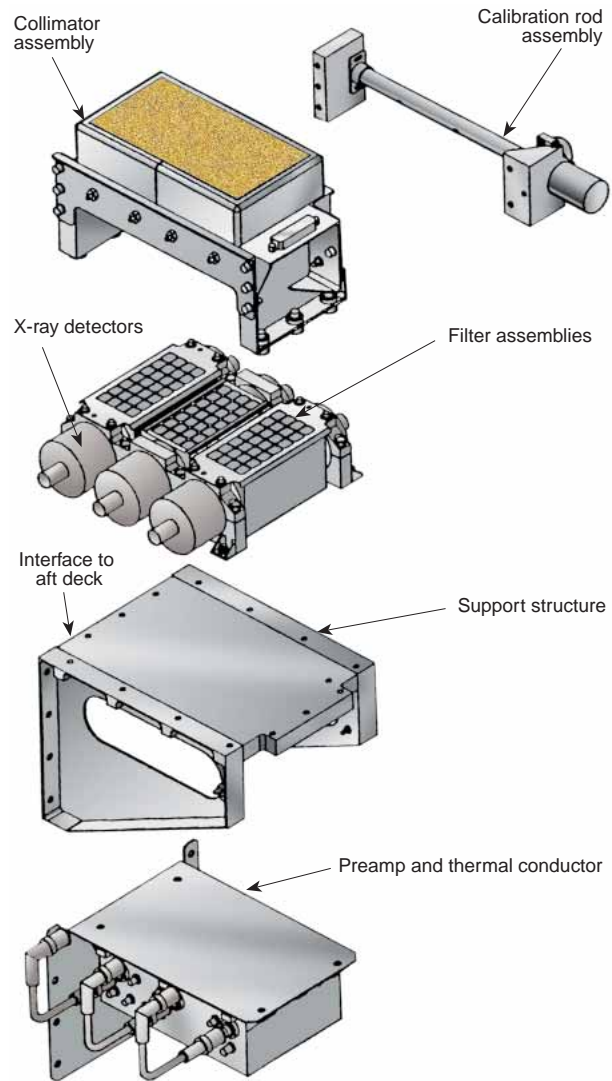


**Figure 6.** Exploded view of the NEAR X-ray sensor assembly.

of the primary peaks. Of course, this effect does not occur for emission lines with energies below 3 keV.

#### Flight Detectors

The flight detectors (Fig. 7) each have a rectangular aperture with an active area of  $25 \text{ cm}^2$ . The window material is beryllium foil,  $25 \mu\text{m}$  thick, supported by an external grid made of solid beryllium. The detector housing is stainless steel with a beryllium liner to absorb fluorescence X-rays arising from the housing itself. The chamber is filled with a gas mixture of 90% argon and 10% methane to an absolute pressure slightly more than 1 atm. The anode wire is gold-plated tungsten with a diameter of  $13 \mu\text{m}$ .

Unlike the gamma-ray detectors, the X-ray gas tubes are not particularly sensitive to temperature and may be operated over a wide temperature range, since

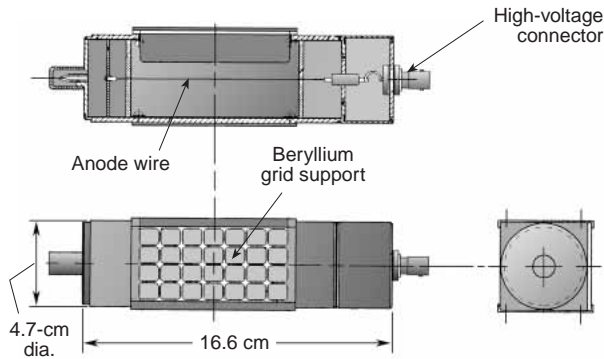


**Figure 7.** Outline (top) and cross-sectional view (bottom) of a NEAR gas-filled proportional X-ray detector.

the multiplication effect depends more on the number of gas molecules than the gas pressure. However, like the gamma-ray PMTs, the gain in the gas tubes is sensitive to voltage variations. To maintain calibration, the XRS shares with the GRS the special feedback control system that maintains ultrastable high-voltage outputs.

The gas proportional counters exhibit a high background from cosmic rays because of their relatively large size (compared with a solid-state detector, for example). To reduce this background, the XRS employs rise-time discrimination circuitry to reject up to 70% of these background events. The cosmic rays usually interact at the walls of the detectors and leave long ionization trails that exhibit characteristically longer charge-collection times. The performance of rise-time rejection is a function of energy and gains little below 2 keV (Mg, Al, Si emission lines occur at 1.25, 1.49, and 1.74 keV, respectively), but significantly improves the signal-to-background ratio at higher energies, especially for weak emission lines such as Fe (6.4 keV).

#### X-Ray Filters

The energy resolution of the gas tubes is not sufficient to resolve the closely spaced Mg, Al, and Si lines. To separate these lines, the XRS uses balanced filters, exploiting the small energy difference between the K $\alpha$  X-ray lines and the K-absorption edge in Mg and Al.<sup>3</sup> An external Mg filter, 8.5  $\mu$ m thick, on one of the outer detectors attenuates the Al line, and a similar Al filter on the other outer detector attenuates the Mg and Si lines. The very steep absorption edges of the filters make the separation of the lower-energy lines possible. At higher energies, the filters are essentially transparent and the Ca and Fe lines are resolved directly by the detectors. The center detector has no filter.

#### X-Ray Collimator

The XRS requires a collimator to provide spatial resolution and eliminate unwanted X-ray sky background. Since the pure beryllium machined collimator used on the Apollo missions was too massive and costly, a compact, honeycomb structure fabricated from Be-Cu foil was substituted for the XRS. Copper is an acceptable material because characteristic Cu X-rays fall above and below the energy line emissions from the asteroid surface (beryllium X-rays all lie below the energy threshold).

To make the collimator, over 50 Be-Cu foils were first corrugated and then hand-assembled using an epoxy containing only light elements. The honeycomb section was then mounted in a sheet-metal frame. The collimator achieves better than 99% transmission, and its small-cell design eliminates the need for precise alignment with the detectors.

#### X-Ray Calibration Rod

To enable calibration verification of the asteroid-pointing detectors, a Vespel rod containing three Fe-55 radioactive sources spans the X-ray detector assembly near the base of the collimator. The bottom edge of the collimator is beveled to allow the rod to rotate the sources into view of the detectors for periodic in-flight calibration without sacrificing active area. An outer copper tube shields the sources when not in use. A stepper motor mechanism at one end directly drives the rod, and a pair of optical reference holes report its position.

The radioactive source holders are embedded axially in the rod, one at each detector location and at 45° from each other so that only one detector can be in calibration at a time. Pinholes in the outer copper tube restrict the photon rate and also act as crude collimators to minimize source cross talk between detectors and ensure maximum science return in the event of a failed mechanism. An in-flight pulse-height spectrum of the Mg-filtered proportional counter with the Fe-55 source in the field of view is shown in Fig. 8.

#### Solar Monitors

The two sunward-pointing X-ray detectors positioned on the forward deck of the spacecraft monitor the incident solar flux. These monitors must possess a wide 60° field of view to observe the Sun continuously throughout the mission. Unlike the asteroid-pointing detectors, which must collect the weak emissions from the asteroid surface, the solar monitors experience the very strong X-ray emissions coming directly from the Sun, especially during solar flares. Therefore, the active area for a solar monitor is only 1 mm<sup>2</sup> compared with the 2500-mm<sup>2</sup> active area of a single gas tube.

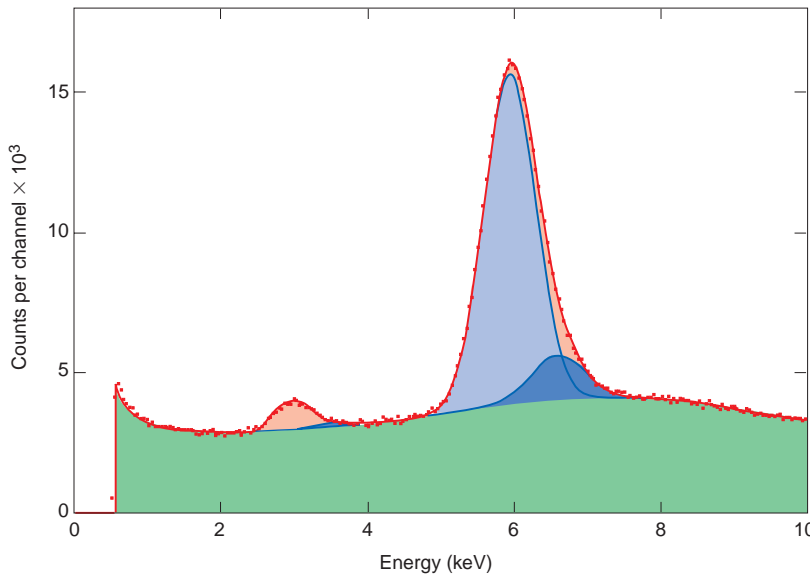


**Figure 8.** Pulse-height spectrum of the Mg-filtered proportional counter with the Fe-55 source in the field of view. The fit to the spectrum (red curve) is accomplished by including the K $\alpha$  (5.89-keV) and K $\beta$  (6.54-keV) emission lines in both the full energy and escape peaks (blue curves) plus a polynomial for the background (green curve). The fit for the full-energy K $\alpha$  line gives a fwhm of 840 eV.

The allowance for a small active area permitted the use of a new miniature X-ray detector developed and built by AMPTEK, Inc. (Fig. 9). The compact sensor consists of a Si-PIN photodiode mounted on a miniature thermoelectric cooler inside a hermetic package that is only 15 mm in diameter. Also mounted on the cooler are the input field-effect transistor and feedback components of the charge-sensitive preamplifier as well as an integrated circuit temperature monitor. A 76- $\mu$ m beryllium window rejects the intense solar flux below  $\sim$ 1 keV. The Si-PIN solar monitor achieves an energy resolution of 600 eV fwhm at 5.9 keV.

Early tests indicated that exposure to ionizing radiation could produce significant damage in the detector. However, subsequent testing demonstrated that the detector would anneal almost completely when heated to 100°C for 24 hours. To address the possibility of radiation damage during the mission, the XGRS contains circuitry to monitor the leakage current of the Si-PIN detector and, if necessary, to reverse the operation of the thermoelectric cooler to provide in-flight annealing.

Since reliance on this new Si-PIN X-ray detector for such a critical function as the solar monitor was considered too risky, a gas proportional counter, identical to the asteroid-viewing ones, is also mounted on the sunward deck. In this case, the large active area of the gas tube needed to be severely restricted. Rather than using a simple pinhole, the gas tube is equipped with a specially designed graded shield made from several layers of progressively denser materials, each with a unique aperture size, to enhance detector

sensitivity at higher energies. At low energies, the shield has an equivalent aperture size of roughly 1 mm<sup>2</sup>. With increasing energy, the higher-density layers become increasingly transparent, opening up the effective area of the detector and increasing its sensitivity. Such a modified energy response is better matched to the solar spectrum that follows a power law and may drop 4 orders of magnitude in intensity from 1 to 10 keV.

Telemetry data may be selected from either solar monitor, or a “toggle mode” can be selected to alternate the data return from each. In this mode, the instrument provides nearly continuous observations from both solar monitors and allows close cross-calibration between the two detectors without increasing the overall instrument data rate. The solar monitors

rely on prominent line emissions from the Sun for in-flight calibration. Figure 10 shows pulse-height spectra obtained in flight with both the gas tube and Si-PIN detectors.

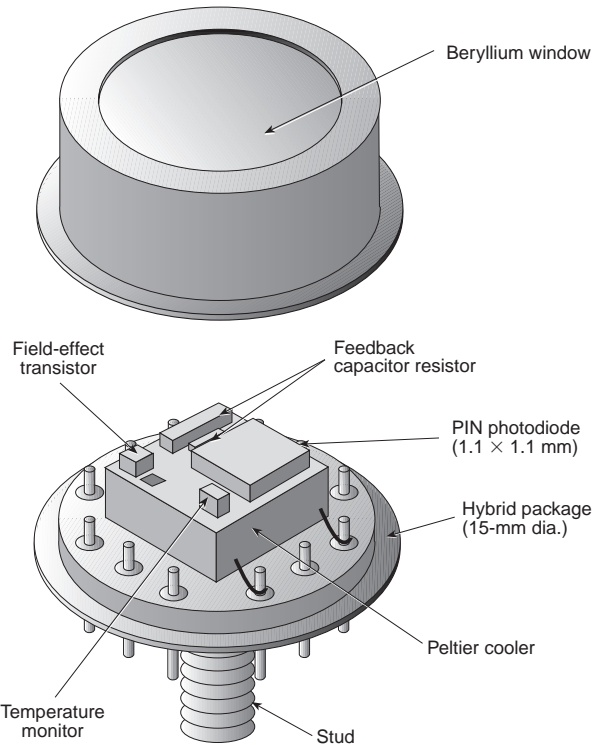


**Figure 9.** Miniature X-ray detector used to monitor solar X-ray flux.

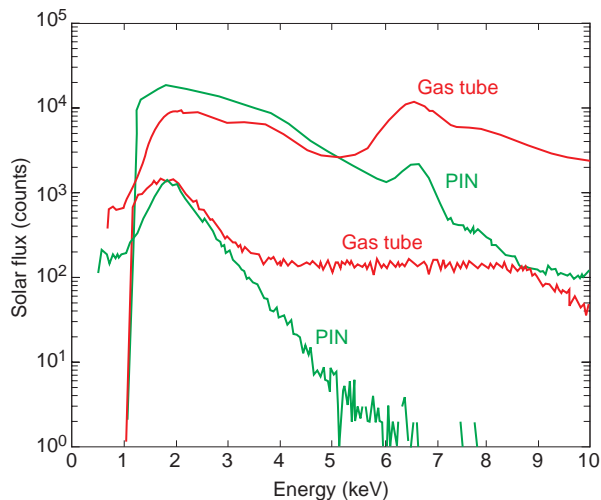


**Figure 10.** A comparison of solar spectra from the gas tube and solid-state solar monitors. The bottom two traces show spectra during a quiescent period. Note the significantly lower background in the solid-state detector (green trace). The upper two traces show spectra during a solar flare. The predominant line near 6.6 keV indicates strong Fe X-ray emissions, nearly 4 orders higher than during quiescent conditions. The gas tube spectrum (red trace) clearly shows the effect of the graded shield in "flattening" the detector response to solar input.

## SUMMARY

The unique measurements provided by the NEAR XGRS will make significant contributions to our understanding of the composition and evolution of 433 Eros and to near-Earth asteroids in general. By remotely sensing characteristic X-ray and gamma-ray emissions, the instrument will provide the first elemental abundance map of a small body. These measurements, which are sufficient to distinguish between major meteorite types, will establish whether there is a chemical relationship between meteorites and the asteroids considered to be their parent bodies.

The design approach of the XGRS enables the instrument to achieve major science objectives in a manner unlike previous instruments, which relied on massive booms, cryogenically cooled detectors, or

expensive beryllium structures. In this way, the XGRS design is consistent with the demanding goals of NASA's Discovery Program to further our knowledge of planetary science using innovative, low-cost missions.

## REFERENCES

- 1 Farquhar, R. W., Dunham, D. W., and McAdams, J. V., "NEAR Mission Overview and Trajectory Design," *J. Astronaut. Sci.* 43(4), 353–371 (Oct-Dec 1995).
- 2 Santo, A. G., Lee, S. C., and Gold, R. E., "NEAR Spacecraft and Instrumentation," *J. Astronaut. Sci.* 43(4), 373–397 (Oct-Dec 1995).
- 3 Trombka, J. I., Boynton, W. V., Brückner, J., Squyres, S. W., Clark, P. E., et al., "Compositional Mapping with the NEAR X-Ray/Gamma-Ray Spectrometer," *J. Geophys. Res.* 102, 23,729–23,750 (1997).
- 4 Clark, P. E., and Trombka, J. I., "Remote X-Ray Spectrometry for NEAR and Future Missions: Modeling and Analyzing X-Ray Production from Source to Surface," *J. Geophys. Res.* 102(E7), 16,361–16,384 (1997).
- 5 Mandel'shtam, S., Tindo, I. P., Cheremukhin, G. S., Sorokin, L. S., and Dmitriev, A. B., "Lunar X Rays and the Cosmic X-Ray Background Measured by the Lunar Satellite Luna-12," *Cosmic Res.* 6, 100–106 (1968).
- 6 Evans, L. G., Reedy, R. C., and Trombka, J. I., "Introduction to Planetary Remote Sensing Gamma Ray Spectroscopy," in *Remote Geochemical Analysis: Elemental and Mineralogical Composition*, C. Pieters and P. Englert (eds.), Press Syndicate of University of Cambridge, Cambridge, England (1993).
- 7 Boynton, W. V., Trombka, J. I., Feldman, W. C., Arnold, J. R., Englert, P. A. J., et al., "Science Applications of the Mars Observer Gamma-Ray Spectrometer," *J. Geophys. Res.* 97, 7681–7698 (1992).
- 8 Egiazarov, B. G., Kononov, B. N., Kurochkin, S. S., Surkov, Yu. A., and Shekhovtsov, N. A., "The Gamma Spectrometer on Luna-10 for the Study of Lunar Rocks," *Cosmic Res.* 6, 223–228 (1968).
- 9 Evans, L. G., Starr, R., Trombka, J. I., Brückner, J., Bailey, S. H., et al., "Performance of the Gamma-Ray Detector System for the NEAR Mission and Application to Future Missions," in *Proc. 2nd IAA International Conference on Low-Cost Planetary Missions*, IAA-L-0905P, Laurel, MD (1996).
- 10 Adler, I., Trombka, J., Gerard, J., Lowman, P., Schmadebeck, R., et al., "Apollo 15 Geochemical X-Ray Fluorescence Experiment: Preliminary Report," *Science* 175, 436–440 (1972).
- 11 Adler, I., Trombka, J., Gerard, J., Lowman, P., Schmadebeck, R., et al., "Apollo 16 Geochemical X-Ray Fluorescence Experiment: Preliminary Report," *Science* 177, 256–259 (1972).

**ACKNOWLEDGMENTS:** The author thanks all XGRS team members for their outstanding performance in developing this instrument and, in particular, APL's Technical Services Department for the tremendous support in meeting the very demanding schedule dictated by the NEAR program. Many thanks also go to Joan Buttermore and Ray Thompson for their fine work in assembling the instrument, Paul Bierman for his dedicated effort on the X-ray collimator, Eric Fiori for his work with the X-ray filters, Dennis Fort for his extensive work on rise-time discrimination, Dave Lohr for the design of the X-ray preamps, John Boldt and Peter Eisenreich for providing a terrific DPU, Susan Schneider and John Hayes for developing uncompromisingly sophisticated and complex flight software, Albert Chacos for providing superb instrument GSE, and, finally, Rob Gold and Hugo Darlington for their general expertise in scientific instruments and helpful nature. This work was supported under contract N00039-95-C-0002 with the U.S. Navy.

## THE AUTHOR



JOHN O. GOLDSTEN received a B.S. from The University of Pennsylvania in 1982 and an M.S. from The Johns Hopkins University in 1986, both in electrical engineering. He joined APL in 1982, and is currently a member of the Senior Staff in the Space Department's Space Sciences Instrumentation Group. He has worked on several space-flight instruments including X-ray and gamma-ray spectrometers, ultraviolet spectrographic imagers, and energetic particle detectors. His e-mail address is john.goldsten@jhuapl.edu.